Intrinsic nonreciprocity in asymmetric Josephson junctions with non-sinusoidal current-phase relations

R. A. Hovhannisyan *

Department of Physics, Stockholm University, AlbaNova University Center, SE-10691 Stockholm, Sweden

(Received 30 March 2025; accepted 4 June 2025; published 18 June 2025)

Josephson junctions (JJs) with nonsinusoidal current-phase relations (CPRs) have gathered increasing attention, partly due to growing interest in topological two-dimensional materials. Understanding how CPRs and inhomogeneities in JJs influence their response is crucial for accurate interpretation of experimental observations. This work reports that a nonsinusoidal CPR, combined with asymmetries in the JJ, can break spatial symmetry and give rise to the Josephson diode effect (JDE) in the short-junction regime. This nonreciprocity is shown to emerge as an intrinsic mechanism related to the maximization of the supercurrent, rather than being solely driven by geometric or material asymmetries. Further analysis shows that JDE efficiency is strongly influenced by the CPR shape but is largely insensitive to junction asymmetry, making the observed nonreciprocity not only a potential experimental signature of unconventional CPRs but also a possible method for probing their properties.

DOI: 10.1103/v41v-1qjw

Josephson junctions (JJs) are characterized by their highly nonlinear response to external stimuli, enabling a range of unique phenomena in superconducting electronics [1–4]. One of the key characteristics of these devices is the current-phase relation (CPR). While the CPR was originally derived to be sinusoidal [5,6], it is now well established that real junctions can exhibit significant deviations from these simpler forms [7–29].

The properties of JJs with nonsinusoidal CPRs under homogeneous magnetic fields and uniform critical current density distributions $J_c(x)$ have been well investigated to date, both experimentally [19,23,30] and theoretically [11,31]. However, in many experimental situations, these ideal conditions are not reproduced due to nonhomogeneities in geometry of the junctions [1,32], quantum Hall effect [33,34], edge states [35], nonuniform current injection [36–38], etc. Although such situations have been considered previously, to my knowledge, no substantial analysis has been conducted on the impact of inhomogeneous current density distributions on the properties of JJs, especially in the long-junction limit.

Another motivation for this study stems from the growing interest in superconducting junctions based on two-dimensional (2D) materials [16–29], which often exhibit unconventional CPRs. Recently, Ref. [39] demonstrated the appearance of the diode effect in an asymmetric superconducting quantum interference device with a nonsinusoidal current-phase relation. Moreover, Ref. [40] reported the experimental observation of nonreciprocal behavior resulting from an asymmetric critical current density in JJs. Nevertheless, the Josephson diode effect (JDE) in 2D materials can also arise from a variety of other mechanisms, including spin-orbit interactions [41,42] or the intrinsic lack of inversion symmetry in the crystal structure [44]. Additionally, external factors like applied magnetic fields [45] or proximity effects in hybrid heterostructures [46] may also contribute to the emergence of nonreciprocal superconducting transport (for more, see the review [47] and references therein). Therefore, the ability to distinguish an asymmetric J_c from other mechanisms is crucial to correctly interpret the observed nonreciprocal behavior.

In this work, I systematically analyze the influence of nonsinusoidal CPRs on the magnetic field dependence of the critical current $I_c(H)$ of the JJ. By exploring both short and long-junction regimes, I find that asymmetries in the critical current density $J_c(x)$, when combined with nonsinusoidal CPRs, lead to nonreciprocal behavior in the short-junction limit. Through a straightforward theoretical analysis, I show that in this regime, nonreciprocity arises as an intrinsic consequence of the critical current maximization mechanism. Further analysis of the JDE, considering both the asymmetry of the junction and the form of the CPR, reveals that while the maximum diode efficiency η is highly sensitive to the shape of the CPR, it can appear in JJs with relatively small asymmetry and is only weakly affected by its degree. This contrast in sensitivity may offer a practical approach for extracting CPR characteristics from measurements of JDE in asymmetric JJs.

I begin by considering the short-junction limit, where the size of the junction can be considered to be smaller than the Josephson penetration depth, i.e. $L \ll \lambda_J$. In this case, one can neglect the screening of the magnetic field by JJ, and the phase shift originating from it can be expressed by the relation

$$\varphi = \frac{2\pi d_{\text{eff}}}{\Phi_0} Hx + \phi \tag{1}$$

*Contact author: razmik.hovhannisyan@fysik.su.se

Published by the American Physical Society under the terms of the Creative Commons Attribution 4.0 International license. Further distribution of this work must maintain attribution to the author(s) and the published article's title, journal citation, and DOI. Funded by Bibsam.

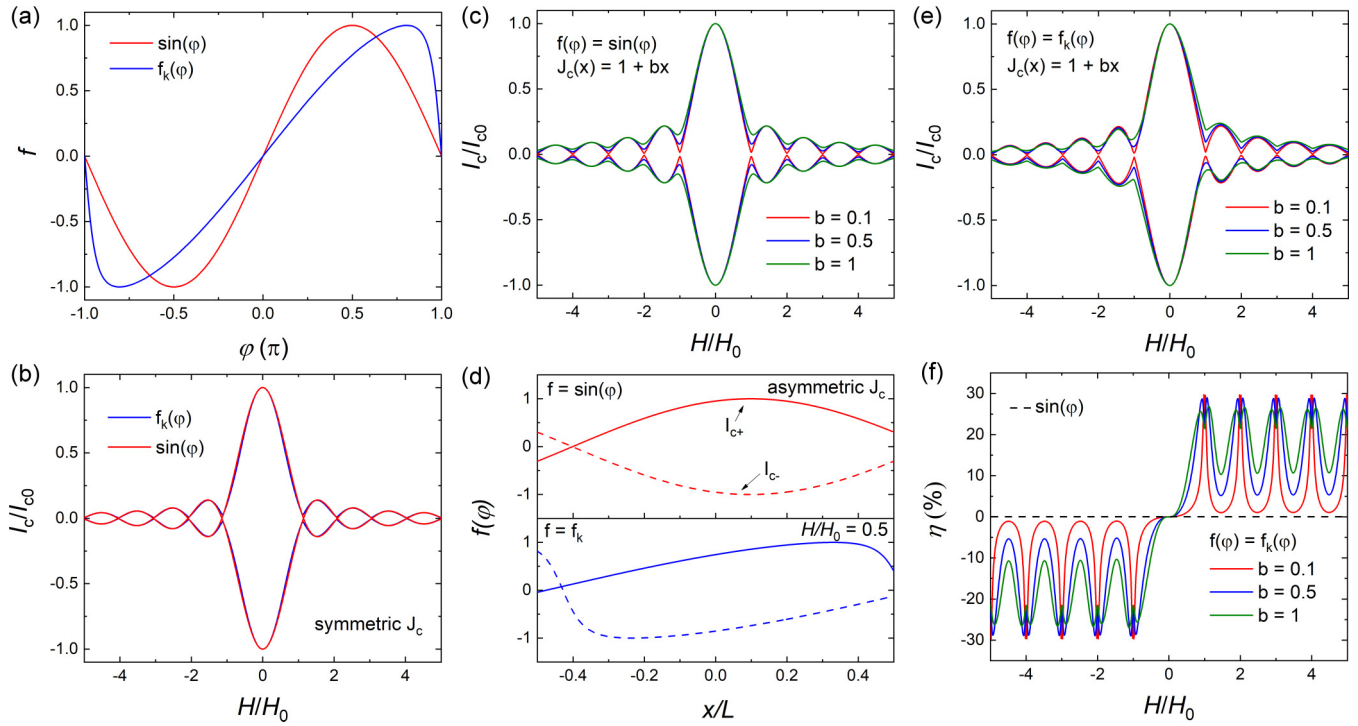


FIG. 1. Diode effect in a JJ with a nonuniform distribution of current density and a nontrivial current-phase relation. (a) CPRs used in the calculations: the sinusoidal CPR described by Eq. (3) (red curve) and the nonsinusoidal CPR given by Eq. (4) (blue curve) corresponding to a transparency parameter $D = 0.99$. (b) Normalized critical current I_c of the JJ as a function of applied magnetic field, computed for a symmetric critical current density profile $J_c(x) = 1 + x^2/L^2$ using the CPRs shown in (a). (c) $I_c(H)$ dependence for an asymmetric critical current density $J_c(x) = 1 + bx/L$ and a sinusoidal CPR. The curves demonstrate the bigger node lifting with increasing b, while preserving both time-reversal and spatial symmetry. (d) Spatial distribution of $f(\varphi)$ for I_{c+} (solid line) and I_{c-} (dashed line) at a magnetic field corresponding to half a flux quantum through the junction, i.e., $H/H_0 = 0.5$, and $b = 0.5$. (e) Critical current I_c as a function of magnetic field for the nonsinusoidal CPR as in (a), and an asymmetric $J_c(x)$ as in (c). The JJ exhibits broken spatial symmetry while preserving time-reversal symmetry. (f) Diode efficiency corresponding to the $I_c(H)$ curves in (e), evaluated as a function of the applied magnetic field. The dashed black curve demonstrate absence of JDE in the case of (c).

where $\Phi_0 = H_0 d_{\text{eff}} L$ is the magnetic flux quantum, d_{eff} is the effective magnetic thickness of the junction, and H is the external magnetic field. The term ϕ in Eq. (1) is an integration constant.

The critical current is then expressed as

$$I_s(H) = \max_{\phi} \left[\int_{-L/2}^{L/2} J_c(x)\, f(\varphi, x)\, \mathrm{d}x \right], \tag{2}$$

where $f(\varphi, x)$ denotes the appropriate CPR, which can take an arbitrary form depending on the properties of the junction [11]. However, for the sake of simplicity, the spatial distribution of the CPR will be neglected.

For further analysis, I focused on two main types of CPRs, shown in Fig. 1(a) and their respective analyses. The first is the ordinary sinusoidal relation

$$f = \sin\varphi. \tag{3}$$

The second corresponds to a generalized form of the CPRs introduced by Haberkorn *et al.* [10], which is applicable to tunnel junctions with arbitrary interface transparency (see also Refs. [11,21,43]):

$$f_k = \frac{\sin\varphi}{\sqrt{1 - D\sin^2(\varphi/2)}}, \tag{4}$$

where D denotes the transparency parameter. The CPR given by Eq. (4) represents a simplified form of the actual CPR at $T = 0$, interpolating between the sinusoidal CPR in the low-transparency limit $D \to 0$, and the clean, high-transparency Kulik-Omelyanchuk limit characteristic of SNS-type junctions with $D \to 1$, where $f \propto \sin(\varphi/2)$ [8].

Figure 1(b) demonstrates the calculated $I_c(H)$ dependencies for a symmetric distribution of $J_c(x) = 1 + x^2/L^2$ (edge state-induced inhomogeneity) for both sinusoidal Eq. (3) and nonsinusoidal Eq. (4) CPRs with transparency parameter $D = 0.99$. It can be observed that, in both cases, the impact of the form of CPR has a negligible effect on the overall shape of the critical current dependence. Only noticeable deference is the appearance of elevated node lifting in the case of nonsinusoidal CPR [43]. During the simulation, I tested a variety of symmetric $J_c(x)$ and $f(\varphi)$ dependencies, and no significant difference was observed. Moreover, the critical currents in the negative and positive direction are equal in amplitude $I_{c+} = I_{c-}$ showcasing no evidence of JDE.

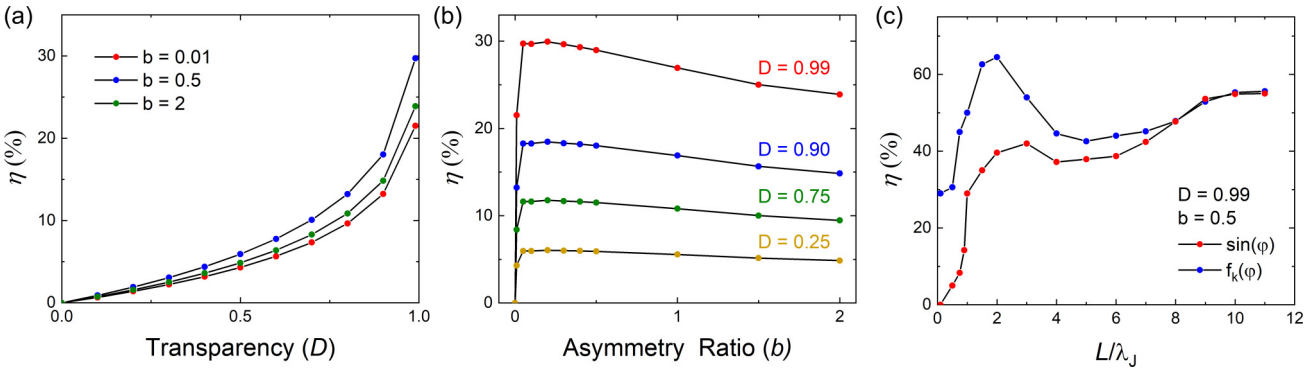


FIG. 2. Dependence of maximum JDE on different junction parameters. (a) Diode efficiency η as a function of the CPR transparency parameter D [Eq. (4)]. A strong increase in η is observed with higher transparency, highlighting the significant impact of the CPR form on nonreciprocity. (b) η as a function of the asymmetry parameter b in the critical current density distribution $J_c(x) = 1 + bx/L$. While a steplike increase in η is visible for small values of b, the overall sensitivity to asymmetry is weak. (c) Diode efficiency η vs normalized junction length L/λ_J. In the short-junction regime ($L/\lambda_J \ll 1$), the nonsinusoidal CPR exhibits residual JDE due to intrinsic mechanisms, while in the long-junction regime ($L/\lambda_J > 9$), both CPRs demonstrate asymptotic diode efficiency (≈55%) driven by self-field (ratchet) effects. The crossover region ($1 < L/\lambda_J < 4$) reveals the complex interplay between intrinsic and self-field mechanisms.

In contrast, Figs. 1(c) and 1(e) present numerically calculated $I_c(H)$ dependencies for an asymmetrical linear distribution of the critical current density, given by $J_c(x) = 1 + bx/L$ (gradient-induced inhomogeneity), for different values of the tilt parameter b.

First, it can be observed that in both cases, the critical current dependencies exhibit significant node lifting, in contrast to the symmetrical $J_c(x)$ [see Fig. 1(b)]. Furthermore, for $f(\varphi) = \sin\varphi$ [Fig. 1(c)], the critical currents I_{c+} and I_{c-} remain equal for any applied magnetic field, indicating the preservation of both spatial and time-reversal symmetries. Indeed, if any $\phi = \varphi_0$ maximizes Eq. (2), then $\varphi_0 + \pi$ minimizes it [see Fig. 1(d), top panel, for the spatial distribution of the $f(\varphi)$ at an applied magnetic field equal to half a flux quantum].

On the other hand, Fig. 1(e) reveals a notable asymmetry in both the critical currents $I_{c+} \neq I_{c-}$ and spatial distribution of phase within the length of the junction, as shown in Fig. 1(d) bottom panel. This leads to a JDE with efficiency

$$\eta = \frac{I_{c+} - I_{c-}}{I_{c+} + I_{c-}}, \tag{5}$$

as demonstrated in Fig. 1(f).

To further investigate the appearance of nonreciprocity in asymmetrical junctions, I have calculated the maximum efficiency, η, reached within the vicinity of the first minimum of the $I_c(H)$ pattern as a function of the CPR [transparency parameter D in Eq. (4)] and the asymmetry ratio b. Figures 2(a) and 2(b) present the results of these calculations respectively. It can be observed that the efficiency exhibits a strong exponential-like dependence on the CPR. Interestingly, unlike the CPR, the maximum achieved nonreciprocity shows a low sensitivity to the asymmetry of $J_c(x)$, displaying a steplike rise in η within the range of $b < 0.05$ and a slowly decaying tail as the total asymmetry increases. Note that the asymmetry of $J_c(x)$ strongly affects the overall behavior of $\eta(H)$ with respect to the magnetic field [see Fig. 1(f)].

Finally, I calculated the diode efficiency dependence in the finite-length junction limit using the sine-Gordon formalism [48,49] for both CPRs (see the Appendix for details). The results are shown in Fig. 2(c). In contrast to the short-junction limit, both CPRs now exhibit significant η, arising from the self-field effects of the JJ; this phenomenon is also known as the vortex ratchet effect [49–52]. For sufficiently long junctions ($L/\lambda_J > 9$), both CPRs converge to an asymptotic efficiency of $\eta \approx 55\%$. However, they start to diverge at smaller L/λ_J, becoming evident for $L/\lambda_J < 4$. The $\sin(\varphi)$ curve peaks at $\eta \simeq 40\%$, while f_k reaches a significantly higher $\eta \simeq 65\%$. As expected, the efficiency of the sinusoidal CPR vanishes as $L \to 0$, while the other retains a residual nonreciprocity of $\eta \simeq 30\%$, consistent with Figs. 2(a) and 2(b).

Thus, I investigate properties of JJs with a nonuniform critical current density $J_c(x)$ and different types of CPRs. To understand the origin of the observed nonreciprocity in the short-junction regime, a careful analysis of Eqs. (1)–(4) is needed. In general, the CPR of a JJ can be written as a sum of Fourier components:

$$f = \sum_{n=1}^{\infty} a_n \sin(n\varphi), \tag{6}$$

where a_n represents the amplitude of each individual Fourier harmonic.

Equation (2) can be solved analytically under the assumption that the discrete Fourier transform of $J_c(x)$ is known for the frequencies defined in terms of the external magnetic field H:

$$A_n = \int_{-L/2}^{L/2} J_c(x) \cos\left(\frac{2\pi d_{\text{eff}}}{\Phi_0} nHx\right) \mathrm{d}x, \tag{7}$$

$$B_n = \int_{-L/2}^{L/2} J_c(x) \sin\left(\frac{2\pi d_{\text{eff}}}{\Phi_0} nHx\right) \mathrm{d}x. \tag{8}$$

Substituting Eq. (6) and the expressions for A_n and B_n into Eq. (2), one obtains

$$I_c(H) = \sum_{n=1}^{\infty} [a_n A_n \sin(n\phi) + a_n B_n \cos(n\phi)]. \tag{9}$$

Furthermore, maximization with respect to the Josephson free phase ϕ reduces to solving a trigonometric equation:

$$\sum_{n=1}^{\infty} [na_n A_n \cos(n\phi) - na_n B_n \sin(n\phi)] = 0. \quad (10)$$

In typical experiments, higher-order harmonics can be neglected. In this case, Eq. (10) is simplified to solving a nth order polynomial equation [31].

Now the appearance of the Josephson diode effect becomes evident. In the case of a symmetric J_c (i.e., an even function of x), the integrand in Eq. (8) becomes an odd function, and thus $B_n = 0$. Additionally, the critical current $I_c(\phi)$, given by Eq. (9), becomes an odd function of ϕ, satisfying $I_c(\phi) = -I_c(-\phi)$. Consequently, if $\phi = \varphi_0$ maximizes the critical current, then $\phi = -\varphi_0$ minimizes it. Furthermore, the integral in Eq. (7) becomes small for any $H \simeq k\Phi_0/Ld_{\text{eff}}$ and a fairly homogeneous $J_c(x)$, due to the inherent 2π periodicity of the integrand. As a result, under these conditions, almost no visible node lifting of the critical current occurs [see Fig. 1(b)].

This reasoning becomes invalid in the case of an asymmetric $J_c(x)$, as the assumption of even symmetry no longer holds. This may lead to nonzero values of B_n, and consequently, to an asymmetric $I_c(\phi)$. Such asymmetry in $I_c(\phi)$ can result in both node lifting and the emergence of JDE. Note that these arguments are not valid for a sinusoidal CPR or any other CPR with translational symmetry, i.e., $f(\varphi) = -f(\varphi + a)$.

Importantly, this mechanism of nonreciprocity is fundamentally different from that in the long-junction regime, as it does not involve self-field effects. This phenomenon is evident from the fact that, unlike in long junctions, the main maximum of $I_c(H)$ in the short-junction regime appears at $H = 0$ [Figs. 1(c) and 1(e)]. The simultaneous presence of nonreciprocity and the absence of self-field effects can be interpreted as a unique signature of a nonsinusoidal CPR in the dependence of $I_c(H)$.

Furthermore, since the maximum diode efficiency is almost independent of the asymmetry in $J_c(x)$ but strongly depends on the CPR, measurements of η can serve as a tool to determine intrinsic properties of the Josephson junction, such as its transparency D.

The substantially different behavior of η within the finite-length junction approximation cannot be explained simply. This is due to a more complex interplay between two mechanisms: self-field and intrinsic. Nevertheless, Fig. 2(c) shows that in the fairly long-junction limit, the self-field mechanism surpasses the intrinsic one, whereas in the short-junction regime, only the intrinsic mechanism is active. Moreover, the overall difference in the transition length within $1 < L/\lambda_J < 4$ of η is approximately 25%, which is close to the residual $\eta \simeq 30\%$ of the intrinsic mechanism between the two CPRs, highlighting this interplay.

To conclude, I examined the impact of the CPR on the properties of a single JJ in both short- and finite-length regimes. In the short-junction limit, it was shown that an asymmetric critical current density leads to a pronounced divergence in $I_c(H)$, which is highly dependent on the CPR and manifests as nonreciprocity in the case of nonsinusoidal CPRs. The theoretical analysis of JDE in this regime, along with its comparison to the finite-length junction approximation, highlights that the effect originates from an intrinsic mechanism, independent of self-field contributions. Furthermore, it was demonstrated that nonreciprocity can arise even in JJs with minimal asymmetry, revealing a distinct fingerprint of the CPR on the critical current modulation. These findings suggest that JDE measurements could serve as a tool for probing intrinsic JJ parameters, such as the CPR.

ACKNOWLEDGMENTS

The author thanks Dr. Denis A. Bandurin, A. Kudriashov, Prof. Vladimir M. Krasnov, and S. Grebenchuk for insightful discussions and valuable feedback that contributed to this work.

DATA AVAILABILITY

The data that support the findings of this article are not publicly available upon publication because it is not technically feasible and/or the cost of preparing, depositing, and hosting the data would be prohibitive within the terms of this research project. The data are available from the authors upon reasonable request.

APPENDIX

The $I_c(H)$ dependencies in the finite-length junction limit were obtained by solving the sine-Gordon equation for the overlap geometry [49]:

$$\frac{\partial^2\varphi}{\partial\bar{x}^2} - \frac{\partial^2\varphi}{\partial\bar{t}^2} - \alpha\frac{\partial\varphi}{\partial\bar{t}} = j_c(\bar{x})f(\varphi,\bar{x}) - j_b(\bar{x}).$$

Here, α is the quasiparticle damping parameter. The normalized critical current density $j_c = J_c/J_{c0}$ and bias current density $j_b = J_b/J_{c0}$ are referenced to the critical current density J_{c0} at $x = 0$. The spatial coordinate is normalized as $\bar{x} = x/\lambda_J$, where the Josephson penetration depth is defined by

$$\lambda_J = \sqrt{\frac{\Phi_0}{2\pi\mu_0 d_{\text{eff}} J_{c0}}}.$$

Time is normalized as $\bar{t} = \omega_p t$, where ω_p is the plasma frequency.

The boundary conditions are given by

$$\left.\frac{\partial\varphi}{\partial x}\right|_{x=0,L} = \frac{2\pi}{LH_0}H,$$

where H is the externally applied magnetic field.

During the calculations, as in the case of short-limit junctions, the spatial dependence of the CPR $f(\varphi,\bar{x})$ was neglected. Furthermore, the asymmetry in the bias current was also disregarded and taken to be uniform.

[1] A. Barone and C. Paterno, *Physics and Applications of the Josephson Effect* (Wiley, New York, 1982).

[2] K. K. Likharev, Superconducting weak links, Rev. Mod. Phys. **51**, 101 (1979).

[3] K. K. Likharev, and V. K. Semenov, RSFQ logic/memory family: A new Josephson-junction technology for sub-terahertz-clock-frequency digital systems, IEEE Trans. Appl. Supercond. **1**, 3 (1991).

[4] R. Bairamkulov and G. De Micheli, Superconductive electronics: A 25-year review, IEEE Circuits and Systems Magazine **24**, 16 (2024).

[5] L. G. Aslamazov and A. I. Larkin, Josephson effect in superconducting point contacts, Pis'ma Zh. Eksp. Teor. Fiz. **9**, 150 (1969) [JETP Lett. **9**, 87 (1969)].

[6] B. D. Josephson, Coupled superconductors, Rev. Mod. Phys. **36**, 216 (1964).

[7] I. O. Kulik, Macroscopic quantization and the proximity effect in SNS junctions, Zh. Eksp. Teor. Fiz. **57**, 1745 (1969) [Sov. Phys. JETP **30**, 944 (1969)].

[8] I. O. Kulik and A. N. Omel'Yanchuk, Properties of superconducting microbridges in the pure limit, Sov. J. Low Temp. Phys. **3**, 459 (1977).

[9] I. O. Kulik and A. N. Omelyanchouk, Current flow in long superconducting junctions, Zh. Eksp. Teor. Fiz. **68**, 2139 (1975) [Sov. Phys. JETP **41**, 1071 (1975)].

[10] W. Haberkorn, H. Knauer, and J. Richter, A theoretical study of the current-phase relation in Josephson contacts, Phys. Status Solidi A **47**, K161 (1978).

[11] A. A. Golubov, M. Y. Kupriyanov, and E. Il'Ichev, The current-phase relation in Josephson junctions, Rev. Mod. Phys. **76**, 411 (2004).

[12] A. V. Galaktionov and A. D. Zaikin, Quantum interference and supercurrent in multiple-barrier proximity structures, Phys. Rev. B **65**, 184507 (2002).

[13] Z. G. Ivanov, M. Y. Kupriyanov, K. K. Likharev, S. V. Meriakri, and O. V. Snigirev, Boundary conditions for the Eilenberger and Usadel equations and properties of "dirty" SNS sandwiches, Sov. J. Low Temp. Phys. **7**, 274 (1981).

[14] M. Y. Kupriyanov, Effect of a finite transmission of the insulating layer on the properties of SIS tunnel junctions, Pisma Zh. Eksp. Teor. Fiz. **56**, 414 (1992) [JETP Lett. **56**, 399 (1992)].

[15] A. I. Buzdin and M. Y. Kupriyanov, Josephson junction with a ferromagnetic layer, Pis'ma Zh. Eksp. Teor. Phys. **53**, 308 (1991) [JETP Lett. **53**, 321 (1991)].

[16] R. C. Dinsmore, M. H. Bae, and A. Bezryadin, Fractional order Shapiro steps in superconducting nanowires, Appl. Phys. Lett. **93**, 192505 (2008).

[17] A. G. P. Troeman, S. H. W. Van Der Ploeg, E. Il'Ichev, H. G. Meyer, A. A. Golubov, M. Y. Kupriyanov, and H. Hilgenkamp, Temperature dependence measurements of the supercurrent-phase relationship in niobium nanobridges, Phys. Rev. B **77**, 024509 (2009).

[18] G. Nanda, J. L. Aguilera-Servin, P. Rakyta, A. Kormányos, R. Kleiner, D. Koelle, K. Watanabe, T. Taniguchi, L. M. Vandersypen, and S. Goswami, Current-phase relation of ballistic graphene Josephson junctions, Nano Lett. **17**, 3396 (2017).

[19] V. S. Stolyarov, D. S. Yakovlev, S. N. Kozlov, O. V. Skryabina, D. S. Lvov, A. I. Gumarov, O. V. Emelyanova, P. S. Dzhumaev, I. V. Shchetinin, R. A. Hovhannisyan, and S. V. Egorov, Josephson current mediated by ballistic topological states in $Bi_2Te_{2.3}Se_{0.7}$ single nanocrystals, Communications Materials **1**, 38 (2020).

[20] C. Kurter, A. D. Finck, Y. S. Hor, and D. J. Van Harlingen, Evidence for an anomalous current–phase relation in topological insulator Josephson junctions, Nat. Commun. **6**, 7130 (2015).

[21] E. M. Spanton, M. Deng, S. Vaitiekėnas, P. Krogstrup, J. Nygård, C. M. Marcus, and K. A. Moler, Current–phase relations of few-mode InAs nanowire Josephson junctions, Nat. Phys. **13**, 1177 (2017).

[22] S. Hart, Z. Cui, G. Ménard, M. Deng, A. E. Antipov, R. M. Lutchyn, P. Krogstrup, C. M. Marcus, and K. A. Moler, Current-phase relations of InAs nanowire Josephson junctions: From interacting to multimode regimes, Phys. Rev. B **100**, 064523 (2019).

[23] S. M. Frolov, D. J. Van Harlingen, V. A. Oboznov, V. V. Bolginov, and V. V. Ryazanov, Measurement of the current-phase relation of superconductor/ferromagnet/superconductor π Josephson junctions, Phys. Rev. B **70**, 144505 (2004).

[24] I. Sochnikov, A. J. Bestwick, J. R. Williams, T. M. Lippman, I. R. Fisher, D. Goldhaber-Gordon, J. R. Kirtley, and K. A. Moler, Direct measurement of current-phase relations in superconductor/topological insulator/superconductor junctions, Nano Lett. **13**, 3086 (2013).

[25] M. Kayyalha, A. Kazakov, I. Miotkowski, S. Khlebnikov, L. P. Rokhinson, and Y. P. Chen, Highly skewed current-phase relation in superconductor–topological insulator–superconductor Josephson junctions, npj Quantum Mater. **5**, 7 (2020).

[26] M. Della Rocca, M. Chauvin, B. Huard, H. Pothier, D. Esteve, and C. Urbina, Measurement of the current-phase relation of superconducting atomic contacts, Phys. Rev. Lett. **99**, 127005 (2007).

[27] L. V. Ginzburg, I. E. E. Batov, V. V. E. Bol'ginov, S. V. E. Egorov, V. I. Chichkov, A. E. E. Shchegolev, N. V. Klenov, I. I. Soloviev, S. V. Bakurskiy, and M. Y. Kupriyanov, Determination of the current-phase relation in Josephson junctions by means of an asymmetric two-junction SQUID, JETP Lett. **107**, 48 (2018).

[28] M. Endres, A. Kononov, H. S. Arachchige, Y. Yan, D. Mandrus, K. Watanabe, T. Taniguchi, and C. Schonenberger, Current-phase relation of a WTe_2 Josephson junction, Nano Lett. **23**, 4654 (2023).

[29] I. Babich, A. Kudriashov, D. Baranov, and V. S. Stolyarov, Limitations of the current-phase relation measurements by an asymmetric dc-SQUID, Nano Lett. **23**, 6713 (2023).

[30] D. Willsch, D. Rieger, P. Winkel, M. Willsch, C. Dickel, J. Krause, Y. Ando, R. Lescanne, Z. Leghtas, N. T. Bronn, and P. Deb, Observation of Josephson harmonics in tunnel junctions, Nat. Phys. **20**, 815 (2024).

[31] E. Goldobin, D. Koelle, R. Kleiner, and A. Buzdin, Josephson junctions with second harmonic in the current-phase relation: Properties of ϕ junctions, Phys. Rev. B **76**, 224523 (2007).

[32] R. A. Hovhannisyan, T. Golod, and V. M. Krasnov, Superresolution magnetic imaging by a Josephson junction via holographic reconstruction of $I_c(H)$ modulation, Phys. Rev. Appl. **20**, 064012 (2023).

[33] S. Hart, H. Ren, T. Wagner, P. Leubner, M. Mühlbauer, C. Brüne, H. Buhmann, L. W. Molenkamp, and A. Yacoby, Induced superconductivity in the quantum spin Hall edge, Nat. Phys. **10**, 638 (2014).

[34] E. Bocquillon, R. S. Deacon, J. Wiedenmann, P. Leubner, T. M. Klapwijk, C. Brüne, K. Ishibashi, H. Buhmann, and L. W. Molenkamp, Gapless Andreev bound states in the quantum spin Hall insulator HgTe, Nat. Nanotechnol. **12**, 137 (2017).

[35] P. Chen, J. Wang, G. Wang, B. Ye, L. Zhou, L. Wang, J. Wang, W. Zhang, W. Chen, J. Mei, and H. He, Asymmetric edge supercurrents in $MoTe_2$ Josephson junctions, Nanoscale Advances **6**, 690 (2024).

[36] M. V. Milošević, A. Kanda, S. Hatsumi, F. M. Peeters, and Y. Ootuka, Local current injection into mesoscopic superconductors for the manipulation of quantum states, Phys. Rev. Lett. **103**, 217003 (2009).

[37] M. R. Samuelsen and S. A. Vasenko, Influence of the bias current distribution on the static and dynamic properties of long Josephson junctions, J. Appl. Phys. **57**, 110 (1985).

[38] M. Y. Kupriyanov, M. M. Khapaev, Y. Y. Divin, and V. N. Gubankov, Anisotropic distributions of electrical currents in high-T_c grain-boundary junctions, JETP Lett. **95**, 289 (2012).

[39] Y. V. Fominov and D. S. Mikhailov, Asymmetric higher-harmonic SQUID as a Josephson diode, Phys. Rev. B **106**, 134514 (2022).

[40] A. Kudriashov, X. Zhou, R. A. Hovhannisyan, A. S. Frolov, L. Elesin, Y. B. Wang, E. V. Zharkova, T. Taniguchi, K. Watanabe, Z. Liu, K. S. Novoselov, L. V. Yashina, X. Zhou, and D. A. Bandurin, Non-Majorana origin of anomalous current-phase relation and Josephson diode effect in $Bi_2Se_3/NbSe_2$ Josephson junctions, Sci. Adv. **11**, eadw6925 (2025).

[41] R. Wakatsuki, Y. Saito, S. Hoshino, Y. M. Itahashi, T. Ideue, M. Ezawa, Y. Iwasa, and N. Nagaosa, Nonreciprocal charge transport in noncentrosymmetric superconductors, Sci. Adv. **3**, e1602390 (2017).

[42] R. Wakatsuki and N. Nagaosa, Nonreciprocal current in noncentrosymmetric Rashba superconductors, Phys. Rev. Lett. **121**, 026601 (2018).

[43] H. Y. Hui, A. M. Lobos, J. D. Sau, and S. Das Sarma, Proximity-induced superconductivity and Josephson critical current in quantum spin Hall systems, Phys. Rev. B **90**, 224517 (2014).

[44] J. K. Kim, K. R. Jeon, P. K. Sivakumar, J. Jeon, C. Koerner, G. Woltersdorf, and S. S. Parkin, Intrinsic supercurrent nonreciprocity coupled to the crystal structure of a van der Waals Josephson barrier, Nat. Commun. **15**, 1120 (2024).

[45] S. Hoshino, R. Wakatsuki, K. Hamamoto, and N. Nagaosa, Nonreciprocal charge transport in two-dimensional noncentrosymmetric superconductors, Phys. Rev. B **98**, 054510 (2018).

[46] H. Narita, J. Ishizuka, R. Kawarazaki, D. Kan, Y. Shiota, T. Moriyama, Y. Shimakawa, A. V. Ognev, A. S. Samardak, Y. Yanase, and T. Ono, Field-free superconducting diode effect in noncentrosymmetric superconductor/ferromagnet multilayers, Nat. Nanotechnol. **17**, 823 (2022).

[47] M. Nadeem, M. S. Fuhrer, and X. Wang, The superconducting diode effect, Nat. Rev. Phys. **5**, 558 (2023).

[48] V. M. Krasnov, Josephson junctions in a local inhomogeneous magnetic field, Phys. Rev. B **101**, 144507 (2020).

[49] V. M. Krasnov, V. A. Oboznov, and N. F. Pedersen, Fluxon dynamics in long Josephson junctions in the presence of a temperature gradient or spatial nonuniformity, Phys. Rev. B **55**, 14486 (1997).

[50] J. E. Villegas *et al.*, A superconducting reversible rectifier that controls the motion of magnetic flux quanta, Science **302**, 1188 (2003).

[51] C. C. de Souza Silva, J. Van de Vondel, M. Morelle, and V. V. Moshchalkov, Controlled multiple reversals of a ratchet effect, Nature (London) **440**, 651 (2006).

[52] J. Lustikova, Y. Shiomi, N. Yokoi, N. Kabeya, N. Kimura, K. Ienaga, S. I. Kaneko, S. Okuma, S. Takahashi, and E. Saitoh, Vortex rectenna powered by environmental fluctuations, Nat. Commun. **9**, 4922 (2018).